# Novelty Detection and 3D Shape Retrieval based on Gaussian Mixture Models for Autonomous Surveillance Robotics

P. Núñez, P. Drews Jr, R. Rocha, M. Campos and J. Dias

***Abstract*— This paper describes an efficient method for retrieving the 3-dimensional shape associated to novelties in the environment of an autonomous robot, which is equipped with a laser range finder. First, changes are detected over the point clouds using a combination between the *Gaussian Mixture Model* (GMM) and the *Earth Mover's Distance* (EMD). Next, the shape retrieval is achieved using two different algorithms. First, new samplings are generated from each Gaussian function, followed of a *Random Sampling Consensus* (RANSAC) algorithm to retrieve geometric primitives. On the other hand, a new algorithm is developed to directly retrieve the shape according to the mathematical space of Gaussian mixture. In this paper the set of geometric primitives have been limited to the set *C = {sphere, cylinder, plane}*. The two shape retrieval methods are compared in terms of computational cost and accuracy. Experimental results in various real and simulated scenarios demonstrate the feasibility of the approach.**

## I. Introduction

Autonomous mobile robot operation in unknown and dynamic environments relies on (1) building a map of the environment based on perceptual data, (2) localizing itself with respect to the map, and (3) autonomous exploration and navigation. Extensive work has been devoted for the past decade to techniques that deal with Simultaneous Localization and Mapping (SLAM), i.e. integrated solutions for the first two problems [1], and also to the action selection problem (e.g. [2]).

For the latter problem, it is important to provide the mobile robot with some kind of alarms that are activated whenever there are important changes in the environment, namely changes that may influence its path. Therefore, when the robot revisits some section of the environment, it is worth to compare current perceptual data with previously acquired data, so as to detect significant changes [3]. The scope of this problem is however not confined to mobile robot navigation. For instance, it is certainly important for automatic surveillance and security systems [4] or, in general, whenever there is a need to compare two signals of the same type with the aim of detecting novelty. Solving the problem in real-time with huge datasets is quite challenging and requires the development of specific techniques. These techniques aim at achieving two inter-related goals (Fig. 1): firstly, to detect whether there is some significant change; secondly, if there is some significant change, to segment the data associated with it.

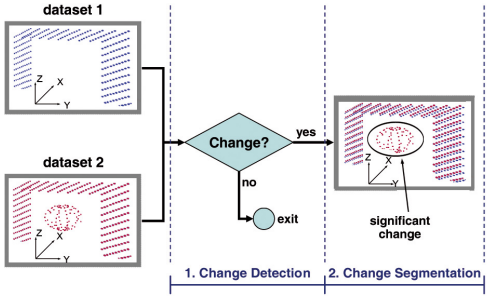


Fig. 1. Change detection and segmentation.

On the other hand, the extraction of geometric shape using 3D point clouds is an important task to obtain a virtual representation of the novelty detected. Such virtual representation provides an abstraction of the point data that eliminates much of the redundancy. Besides, primitive shapes can easily be assembled into higher semantic level models that represent dynamic elements of the environment, e.g. persons, boxes or other robots, and improve the later tasks, as tracking or SLAM. In this work, the set of primitive shapes has been limited to three basic ones, sphere, cylinder and plane. Complex models are a combination of these primitive shapes [5]. Two different methods are developed in this work. The first one is based on the recent work of Schnabel et al. [5], but applied to the 3D scan data acquired by an autonomous robot. Here, we directly re-sample points using the mixture of Gaussians and after applying a RANSAC algorithm to match the set of points to a geometry primitive. In other words, the approach uses samples generated by the GMM in the Euclidean Space and try to match them to a known shape. On the other hand, the mathematical space of Gaussian mixtures is used in the second approach. Covariance and mean of each Gaussian function associated to a novelty are compared with three geometric primitives according to their ideal covariance and mean. Results of this second method are the geometric primitives and rigid transformations that minimize the distance between the two covariance matrices.

The rest of the paper is organized as follows: after briefly showing the state of art of the novelty detection and shape retrieval algorithms in Section II, Section III introduces the

This work has been partially supported by the IRPS, EU-FP6-IST-045048 project, by the Spanish Ministerio de Ciencia y Tecnología (MCYT) Project n. HP2005-01359 and FEDER funds.

P. Núñez is member of the ISIS Group, Dpto. Tecnología Electrónica, Universidad de Málaga, and is with Dept. Tecnología de los Computadores y las Comunicaciones, Universidad de Extremadura, Spain (e-mail: pmnt@uma.es).

M. Campos is with Dept. Computer Science Federal University of Minas Gerais, Brazil.

Rest of authors are with the Institute of Systems and Robotics, Dept. Electrical and Computer Engineering, University of Coimbra, Portugal.

change detection algorithm. The two proposed algorithms for shape retrieval are presented in Section IV. Experimental results in Section V demonstrate the efficiency and precision of the proposed method. Finally, in Section VI, the main conclusions of this approach and future work are drawn.

## II. Related work

The proposed approach presents an efficient method for change detection in the robot's environment and the 3-D shape retrieval associated to it. The behavior of an autonomous mobile robot working in dynamic environments has been intensively researched in the last years. The basic idea behind most of the current navigation systems operating in a dynamic environment treat to remove the dynamic objects in order to improve the navigation and localization tasks [6], [7]. However, these changes in the robot's surrounding are able to be interesting depending of the applications. Thus, Andreasson *et al.* presented a system for autonomous change detection with a security patrol robot [4]. The system uses 3D laser range data and a color camera to build a reference model of the environment and then discover changes with respect to that reference model using SIFT features.

Related to the proposed approach, in [3], three different computational techniques for novelty detection were experimentally compared in terms of their novelty discriminating power. Gaussian Mixture Models (GMM) presented the most consistent behavior. Furthermore, a generic metric to quantify changes was formulated by using Earth Mover's Distance (EMD), a distance metric between two data distributions.

On the other hand, the detection of primitive shapes is a common task in many areas of geometry related computer science. Along the last decades, a vast number of algorithms has been proposed. Some authors used the well-known Hough's transform [8] to obtain the shape, but they have a high computational cost to compute 3D information. Other techniques are based on a region growing [9], which use a seed region in the scan data and is then grown into neighboring areas. In the recent years, some authors have proposed RANSAC-based shape detection method [10], [5], which is a robust method for shape retrieval. An excellent review of these methods can be found in [11].

## III. Novelty detection Algorithm in 3-D maps

The two main steps of novelty detection depicted in Fig. 1 in general terms are further detailed in Fig. 2 when using both GMM and EMD [3]. Firstly, data in Euclidean space is transformed to the mathematical space of GMM, so as to achieve data compression and efficient comparison using the EMD-based quantification of novelty. Secondly, if this quantification is above a given threshold, data associated with novelty is segmented in GMM space and back-propagated to the Euclidean space using the shape retrieval algorithm. The main advantages of using the GMM space is that it enables an efficient fusion of point clouds, and that its dimensionality is small. A brief description of the novelty detection algorithm is explained in the next subsections.

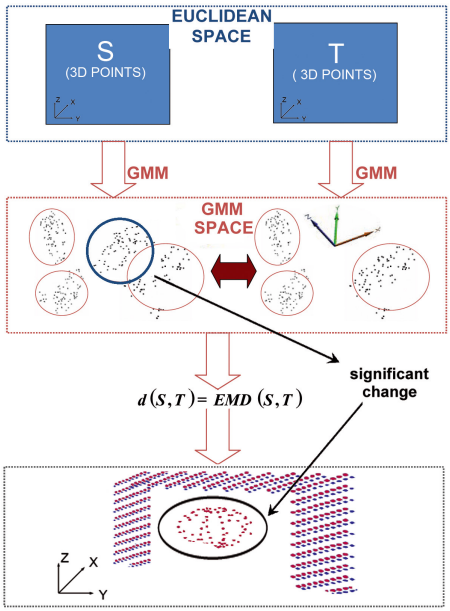


Fig. 2. Two main steps of novelty detection and shape retrieval algorithm proposed in this paper: novelty detection and segmentation using GMM and EMD; and the shape retrieval of the detected changes.

### A. Mixture of Gaussian functions

A *mixture of Gaussian functions* is a probability density function described by a convex linear combination of Gaussian density functions [12]. Therefore, a function is a mixture of Gaussian functions if it has the form:

$$f(\mathbf{x}, \Theta) = \sum_{k=1}^{K} p_k \, g(\mathbf{x}; \mu_k, \Sigma_k) \quad \left(\mathbf{x} \in \mathbb{R}^N\right) \tag{1}$$

where the functions $g$ are Gaussian densities which are defined by $\mu_k \in \mathbb{R}^N$ and $\Sigma_k$, means and the covariance matrices, respectively, and the coefficients $p_k$, known as the *mixing probabilities*, which satisfy:

$$p_k \geq 0 \qquad \text{and} \qquad \sum_{k=1}^{K} p_k = 1. \tag{2}$$

Mixtures of Gaussian functions provide good models of clusters of points: each cluster corresponding to a Gaussian density with mean somewhere in the centroid of the cluster, and with a covariance matrix somehow measuring the spread of that cluster. Conversely, given a set of points in $\mathbb{R}^N$, one can try to find the mixture of Gaussian functions $\Theta$ with a certain number of addends that best fits those points, using a method known as *Expectation Maximization* (see section 2.3 in [12]). For the purpose of this paper, $\Theta$ denotes the $K(1+N+N^2)$ dimensional vector containing all the parameters of the given Gaussian mixture:

$$\Theta = ((\theta_1, p_1), \ldots, (\theta_K, p_K)) \tag{3}$$

where

$$\theta_k = (\mu_k, \Sigma_k) \tag{4}$$

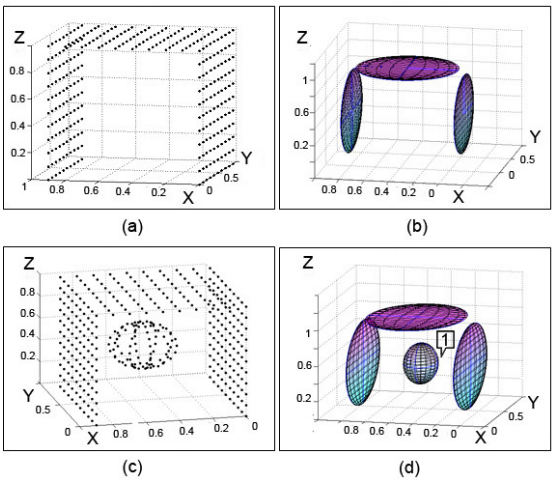


Fig. 3. Novelty detection algorithm: a) ideal 3-dimensional corridor; b) Mixture of Gaussian functions associated to a); c) an object has been moved inside of the corridor; and d) Mixture of Gaussian functions associated to c). The novelty detected by the algorithm has been indicated.

is a vector containing all the coordinates of the means $\mu_k$ and all the entries of the covariance matrix $\Sigma_k$. The conditions in Eq. (2) guarantee that $f$ is indeed a density function. Fig. 3a-c illustrate clouds of 3-D points, which describe an ideal corridor where one object has been moved inside. The mixture of Gaussian functions obtained has been shown in Fig. 3b,d. 3-dimensional Gaussians ($N$ = 3) have been detected, each one is associated to the clusters of points (walls, ceiling and the dynamic object).

### B. Earth Mover's Distance

The *earth mover's distance* (EMD) is defined in [13] as a sort of distance between two distributions of points in space for which a distance between points is given. Reliably, the EMD distance between two sets of points, $A$ and $B$, is calculated as

$$\text{EMD}(A,B) = \min_{F \in \mathcal{F}(A,B)} \frac{\sum_{i=1}^{m}\sum_{j=1}^{n} f_{ij} d_{ij}}{\min\{W,U\}} \qquad (5)$$

where

$$A = \{(x_1,w_1),(x_2,w_2),...,(x_m,w_m)\}$$
$$B = \{(y_1,u_1),(y_2,u_2),...,(y_n,u_n)\}$$

are two sets of $n$-dimensional weighted points, with $m \leq n$, and total weight defined as

$$W = \sum_{i=1}^{m} w_i \quad \text{and} \quad U = \sum_{j=1}^{n} u_j$$

and $d_{ij}$ is the distance from $x_i$ to $y_j$, and $F = \{f_{ij}\} \in \mathcal{F}(A,B)$, with $\mathcal{F}(A,B)$ being the set of all feasible flows between $A$ and $B$ [13].

Therefore, let $\Theta = ((\theta_1,p_1),\ldots,(\theta_n,p_n))$ and $\Gamma = ((\gamma_1,p_1),\ldots,(\gamma_m,p_m))$ being two mixture of Gaussian functions, associated to two 3-dimensional scan data. In order to measure the presence of changes in the environment, we model each Gaussian function as weighted points $(\theta_i,p_i)_\Theta$ and $(\gamma_j,q_j)_\Gamma$, being $\theta_i$ and $\gamma_j$ mixture of Gaussian functions, and $p_i$ and $q_j$ the weights associated to this. Thus, the distance between the mixtures of Gaussian is calculated as [3]:

$$d_{GMM}(\mathbf{\Theta},\mathbf{\Gamma}) = \text{EMD}\left(\{(\theta_{1\ldots n},p_{1\ldots n})\},\{(\gamma_{1\ldots m},q_{1\ldots m})\}\right) \qquad (6)$$

**Algorithm 1** Change segmentation algorithm

1: $d_{GMM} \leftarrow EMDdistance(\Theta,\Gamma)$
2: $\Pi \leftarrow 0$
3: **while** $(d_{GMM} \geq U_{th})$ **do**
4: $\quad x(\Sigma,\mu) \leftarrow SelectGaussianfromGMM(\Theta)$
5: $\quad \Pi \leftarrow \Pi \cup x(\Sigma,\mu)$
6: $\quad \Theta \leftarrow \Theta - x(\Sigma,\mu)$
7: $\quad d_{GMM} \leftarrow EMDdistance(\Theta,\Gamma)$
8: **end while**
9: **return** $\Pi$

### C. Novelty segmentation to a mixture of Gaussian

Eq. (6) can be used as a quantitative metric to detect changes in the environment. To do that, a threshold value $U_{th}$ has been defined, which represents the maximum value for consider a novelty between the two maps [3]. Therefore, the algorithm identifies a novelty in the robot's environment iff

$$d_{GMM} \geq U_{th} \qquad (7)$$

Next, a segmentation process is used to segment these changes in a mixture of Gaussian functions. The overall structure of the method is outlined in pseudo-code in algorithm 1. In each iteration, the algorithm selects a $x(\mu,\Sigma)$ feature from $\Theta$ with the greatest quantified change, showed by the function *SelectGaussianfromGMM*. This feature, which is also described by a mixing probability $p$, is removed from the initial mixture $\Theta$ and is also included in the new Gaussian mixture model $\Pi$. The two subsets, $\Theta$ and $\Pi$ are recalculated to obtain the new values of the mixing probability. Besides, the new mixture of Gaussian is used to obtain a new value of the distance $d_{GMM}$. The algorithm returns the mixture of Gaussian functions $\Pi \subseteq \Theta$, which identifies the changes in the 3-dimensional map.

Fig. 3 was used to illustrate the mixture of Gaussian functions associated to 3-dimensional cluster of points. After applying the proposed algorithm between these two sets of Gaussian, a novelty is detected in the maps (marked as 1 in Fig. 3d).

## IV. 3-DIMENSIONAL SHAPE RETRIEVAL

This Section introduces the 3D shape retrieval algorithms used to obtain a model of the detected novelties. Previous stage obtains a mixture of Gaussian functions, which is related to changes identified in the environment. Let $\Pi$ = $((\Pi_1,p_1),\ldots,(\Pi_K,p_K))$ be the vector containing the parameters of this Gaussian mixture, which was described

in detail in Section III, where $\Pi_k = (\mu_k, \Sigma_k)$ is the means and covariance matrices associated to the novelty cluster of points, and $K$ the number of identified novelties. Next, two methods are presented which achieve the 3-dimensional shape retrieval according to this information. In this paper, three basic geometric primitives have been used to model novelties, i.e. sphere, cylinder and plane. The first of the methods uses the Euclidean space to generate the shape. Therefore, the mixture of Gaussian functions is used to generate a 3-D points around the identified changes, which are afterwards modeled using a RANSAC algorithm. The second method presents a new strategy to recover a model of the novelty. Thus, the mathematical space of Gaussian mixture is directly used to achieve this shape retrieval. These two methods will be detailed in the next subsections.

### A. Shape retrieval using Euclidean Space

The Gaussian mixture function is a generative model. In other words, it is useful to consider the process of describing a synthetic 3D region using the samples generated from the Gaussian functions. First, one of the samples $s$ is selected at random with prior probability $p_k$. Next, a data point is generated from the corresponding density $\Pi_k$. The corresponding posterior probabilities, $P(k, x)$, can be written using Bayes' theorem, as

$$P(k, x) = \frac{g(\mathbf{x}; \mu_k, \Sigma_k) \cdot p_k}{f(x, \theta)} \tag{8}$$

where $f(x, \theta)$ is given in Eq. 1. These posterior probabilities satisfy the constraints

$$\sum_{k=1}^{K} P(k \mid x) = 1 \qquad \text{and} \qquad 0 \leq P(k \mid x) \leq 1 \tag{9}$$

By selecting the number of components $N$ to sample, it is possible to control the complexity of the synthetic region. In order to improve the shape retrieval algorithm, generated samples are located on the surface of the novelty. Let $\Sigma_k$ be the covariance matrix associated to the Gaussian. Eigenvectors of this matrix are used to determine the three principal directions of the ellipsoid associated to $\Sigma_k$. On the other hand, eigenvalues of this matrix are used to calculate the lengths of these axes from $\mu_k$. Therefore, the resulting samples are generated over the surface of this ellipsoid. Fig. 4b shows the 3-D points clouds generated in the process of sampling. In this case, the Gaussian mixture is composed of two components, which are illustrated as ellipsoids in the Fig. 4a.

Let $S = \{s1, \ldots, s_N\}$ be the set of synthetic 3-dimensional points generated in the previous step. The RANSAC algorithm is applied to this synthetic set to detect the geometric shape of the novelties in the map. The RANSAC paradigm is a well-known strategy to extract shapes from 3D cloud of points by randomly drawing minimal sets from the data. The resulting candidates shapes are tested against all the points in the data to determine how many of the points are well approximated by the primitive. After a given number of trials, the shape which approximates the most of the points is extracted and the algorithm continues on the remaining data. Our method used the RANSAC algorithm provided by [5], an efficient implementation for recovering the shape of point clouds. The output of the algorithm is a set of primitive shapes $\Psi = \{\Psi_1, \ldots, \Psi_n\}$, with corresponding disjoint set of points $S_{\Psi_1} \subset S$, ..., $S_{\Psi_1} \subset S$ and a set of outliers $R = S \setminus \{S_{\Psi_1}, \ldots S_{\Psi_1}\}$. A detailed description of the algorithm is given in [5]. In this work, the possible shapes has been limited to the set $\Psi_{shape} = \{sphere, cylinder, plane\}$. Fig. 4c illustrates the results (in blue color) of the algorithm in the example of Fig. 4a. The Fig. 4d shows another example to represent a cylinder, in blue color the shape generated when the covariance $\Sigma_k$ is associated to an ideal cylindric novelty. It is appreciated, there is an orientation error in the shape retrieved using Euclidean space, which is due to the loss of information after generating samples from GMM.

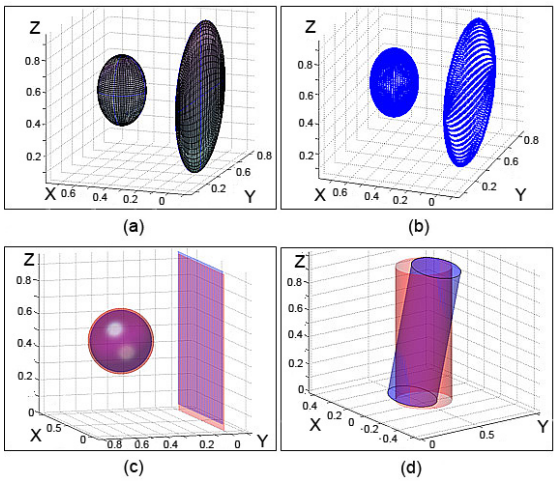


Fig. 4. Shape retrieval algorithms: a) two Gaussian functions which describe the novelty in the 3-dimensional map; b) cloud of points generated by the sampling method; c) retrieved shape according to the first method (Euclidean space, in blue color) and second method (Mathematical space of Gaussian mixture, in red color) for the example a); and d) retrieved shape for a Gaussian function associated to an ideal cylinder.

### B. Shape retrieval based on covariance matrices matching

The shape retrieval algorithm finds the shape that better approximate to an ideal basic shape from $\Psi_{shape}$. To do that, the strategy adopted in this second method uses the mathematical space of the Gaussian mixture model, which is described by the covariance and mean of the Gaussian functions. Let $\Pi$, denote the mixture Gaussian associated to the changes identified in the map. As it was described in Section III, each novelty $k$ is characterized by a Gaussian function, $\Pi_k = (\mu_k, \Sigma_k)$. This paper proposes a new shape retrieval algorithm based on the covariance matrices matching. The algorithm is summarized in Algorithm 2. The best model of the shape and the rigid transformation with respect to an ideal shape, $T$, are the goals of this algorithm. Gaussian functions are matched with each basic

**Algorithm 2** Shape retrieval algorithm (Feature space)

1: $\Psi \leftarrow 0$
2: $T \leftarrow 0$
3: $N_{SHAPE} \leftarrow 3$
4: **for** $i = 1$ to $N_{SHAPE}$ **do**
5: **for** $j = 0$ to $K$ **do**
6: $[d_\Psi^j, \Psi^j, T^j] \leftarrow covarianceDistance(\Sigma_j, \Sigma_i)$
7: **end for**
8: $(\Psi_i, T_i) \Leftarrow getBestShape(d_\Psi)$
9: $\Psi \leftarrow \Psi \cup \Psi_i$
10: $T \leftarrow \Psi \cup T_i$
11: **end for**
12: $\mathbf{return}(\Psi, T)$

shape, measuring the similarity between their covariance matrices, $d_\Psi = \{d_{sphere}, d_{cylinder}, d_{plane}\}$. The minimum value of $d_\Psi$ determines the shape that best approximates to the cloud of points, just as the rigid transformation (line 8 in the algorithm).

Covariance matching is a basic task in measurement design [14]. The goal is to obtain a distance measure of two covariance matrices. The space of covariance matrices is not a vector space and therefore a standard arithmetic difference does not measure the difference between them. But covariance matrices are symmetric and positive semi-definite and then can be formulated a distance based on Riemannian metric. In this paper, the distance metric described by Foerstner and Moonen [14] has been used, which is defined as

$$d(\Sigma_1, \Sigma_2) = \sqrt{\sum_{i=1}^{N} ln^2 \lambda_i(\Sigma_1, \Sigma_2)} \tag{10}$$

where $\Sigma_1$ and $\Sigma_2$ are the two input covariance matrices, $\lambda$ represents the generalized eigenvalues of $\Sigma_1$ and $\Sigma_2$, and N is the dimensionality of the matrices. In this paper, $\Sigma_1$ is the covariance of the Gaussian function which identify a novelty and $\Sigma_2$ is the covariance of a basic shape, i.e. sphere, cylinder or plane. To consider possibles rotations and scaling changes of the model, it must be noted that

$$\Sigma_i = T\Sigma_j T^T = (R \cdot L)\Sigma_j (R \cdot L)^T \tag{11}$$

where $T$ represents the Rigid Transformation applied to the ideal geometric shape (neither scaling nor rotation), which is composed of scaling and rotation matrices, $R$ and $L$. In the proposed approach, the translation is directly known with the mean information of each Gaussian.

$$R = \begin{bmatrix} c\psi c\varphi - c\vartheta s\varphi s\psi & c\psi s\varphi + c\vartheta s\varphi s\psi & s\psi s\vartheta \\ -s\psi c\varphi - c\vartheta s\varphi c\psi & -s\psi s\varphi + c\vartheta c\varphi c\psi & c\vartheta s\psi \\ -s\vartheta s\varphi & -s\vartheta c\varphi & c\vartheta \end{bmatrix} \tag{12}$$

$$L = \begin{bmatrix} L_x & 0 & 0 \\ 0 & L_y & 0 \\ 0 & 0 & L_z \end{bmatrix} \tag{13}$$

being $\psi$, $\vartheta$, $\varphi$, the roll, yaw and pith angles, respectively, $c$ and $s$ the diminutives of cosine and sine mathematical functions, and $L_i$ the scaling factor for each axis.

It is possible to minimize Eq. (10) using a Least squares minimization method based on Levenberg-Marquardt algorithm, which modifies the rotation and scaling matrices in each iteration. A starting guess of the parameters is required to reduce the number of iterations needed to converge and remove local minima situations. To do that, the algorithm uses a good approximation to the rigid transformation $T$ according to the eigenvectors values of the two covariance matrices. Fig. 4c-d represent the retrieved shape (in red color) using this second method.

## V. Experimental Results

The accuracy and computational load of the novelty detection algorithm was tested in our previous work [3]. The authors demonstrated that the GMM-EMD technique is a stable method, in the sense that it presents a lower sensitivity to errors and is able to detect changes with greater reliability.

In this paper, the proposed method has been evaluated using simulated and real data. The algorithms and simulated data were programmed in Matlab software, and the benchmark tests were performed on a PC with a 1.6GHz Intel Core2 CPU. The number of samples generated by the shape retrieval algorithm based on Euclidean space was 3722. The artificial data is formed by a set of 400 points in 3-dimensional space, simulating the readings of a perfect laser range finder in a corridor. A random error, normally distributed with zero mean and variance 0.001, was added to these points. In order to evaluate the algorithm, objects, i.e. cylinders, spheres and planes, are introduced in different poses and with different scale inside the corridor (red color in Fig. 5a-c). A total of 100 different simulated data for each object have been generated for testing.

On the other hand, the real data has been acquired by an Hokuyo laser range finder which is mounted on a Directed Perception pan-tilt unit. Three different data acquisition areas were used at Instituto de Sistema e Robotica's research laboratory (Figs. 6a-c). The experiments consisted on two captures for each test area. First, a 3-D map was acquired to obtain a first representation of the environment. Afterwards, a novelty was introduced, which is drawn in red color in Figs. 6d-f (an opened door, a person in the corridor and a closed door, respectively). The size of these objects was known, and the pose was also calculated using an inertial sensor coupled to them and the robot pose. Finally, in order to obtain statistical results, the experiments were repeated ten times for each test area.

The experimental results are focused on the accuracy and processing time of the proposed shape retrieval strategies. Thus, the accuracy measurements for both, simulated and real data, have been defined as

TABLE I

COMPARATIVE STUDY FOR SIMULATED DATA.

| Algorithm | Euclidean Space | Feature Space |
|---|---|---|
| Execution time (sec) | 0.3491 | 0.07425 |
| TruePos | 0.8330 | 0.9367 |
| FalsePos | 0.1467 | 0.0400 |
| $\sigma_{\Delta S(S_x,S_y,S_z)}$ [cm] | (12.13, 11.01, 8.09) | (9.11, 7.998, 7.11) |
| $\sigma_{\Delta R(\psi,\vartheta,\varphi)}$ [deg] | (2.01, 1.12, 3.22) | (1.32, 1.99, 2.88) |

TABLE II

COMPARATIVE STUDY FOR REAL DATA.

| Algorithm | Euclidean Space | Feature Space |
|---|---|---|
| Execution time (sec) | 0.3231 | 0.3156 |
| TruePos | 0.8667 | 0.9000 |
| FalsePos | 0.0667 | 0.0667 |
| $\sigma_{\Delta S(S_x,S_y,S_z)}$ [cm] | (16.21, 13.24, 10.55) | (12.12, 6.22, 8.19) |
| $\sigma_{\Delta R(\psi,\vartheta,\varphi)}$ [deg] | (4.21, 3.98, 5.12) | (3.12, 2.01, 3.02) |

$$TruePos = \frac{NumberTrueShapes}{NumberShapes}$$
$$FalsePos = \frac{NumberErrShapes}{NumberShapes} \quad (14)$$

where $NumberTrueShapes$ is the number of retrievals to true shapes, $NumberShapes$ is the total number of shapes detected by the algorithm, and $NumberErrShapes$ is the number of retrievals to false shapes. To determine the precision, the shapes obtained by the algorithms have been compared to the real pose and scale of the objects inside the corridor. The results were automatically checked and classified in Tables I and II.

### A. Simulated data

Results after applying the algorithms to the simulated data are summarized in Table I. As can be appreciated, average computational load of the two algorithms are different, because the time of RANSAC depends of the number of the points and in the our method depends on the difference in scale and rotation between the standard shape and the shape to be retrieved. This computation time includes the whole process, that is, the change detection, segmentation and the shape retrieval. Computational time has been determined using the compiled file in Matlab. Results for the three typical observations in Fig. 5a-c are in Fig. 5d-f, where examples of true and false positives are illustrated for particular cases. The Gaussian mixture functions were correctly classified to their shapes (true positives) in 0.833 cases for the first algorithm and 0.9367 for the second method. On the contrary, non-corresponding Gaussian functions were erroneously reported as shapes (false positives) in 0.1467 and 0.0400 cases, respectively. The main reasons for failure were: a) error in the EM algorithm, due to the proximity of the clusters of points; b) poorly representation of the covariance matrix; and c) ambiguous covariance matrix associated to the clouds of 3-dimensional points. Furthermore, the average error associated to the retrieved shape is higher for the algorithm that uses the re-sampling and RANSAC methods [1].

### B. Real data

Table II illustrates the results of the proposed algorithms using real data. Due to the reduced number of experiments, statistical results differs from the simulated data. It is appreciated that the processing time results are higher than simulated data, which is due to the number of points to process.

[1]It is necessary to comment that the worse results for the RANSAC method were obtained when the synthetic object was a cylinder

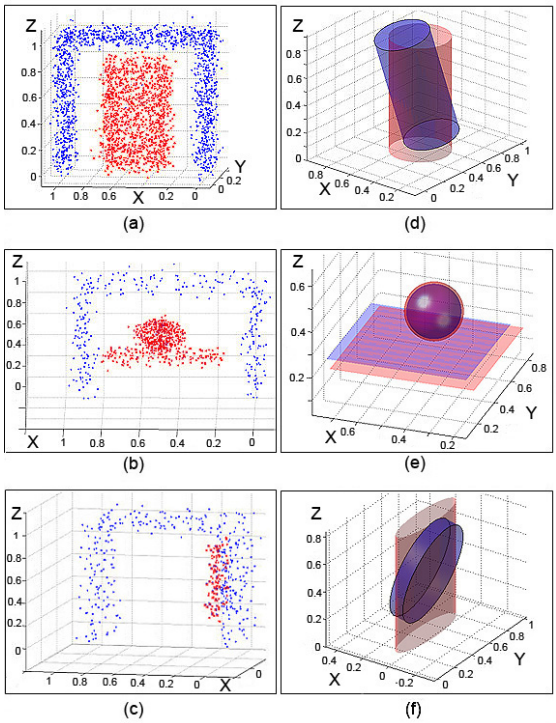


Fig. 5. Simulated data for testing the shape retrieval algorithms: a-c) Simulated observations from an ideal laser to a corridor and an object inside of it. d-f) Shapes generated by the algorithms (blue: method based on Euclidean space; red: method based on Mathematical space of Gaussian mixture). The test f) presents a typical error due to a mistake in the segmentation process , which groups in the same Gaussian function the wall of the corridor and the novelty.

Furthermore, the accuracy of the two proposed approaches decreases for real data. The main reason is the non-ideal shape of the objects respect to the set of primitives used by the algorithms. Nevertheless, the feasibility of the approach for the purpose of this paper has been demonstrated. Results from three typical observations (Figs. 6a-c) are drawn in Figs. 6j-l (Gaussian functions associated to the novelty have been drawn in Figs. 6g-i).

## VI. CONCLUSIONS AND FUTURE WORK

This paper has presented a new method to directly detect changes in the environment of a robot using a 3-D laser range finder and retrieve its shapes using two different methods. *Gaussian Mixture Model* has been used to obtain a new representation of the point clouds and *Earth Mover's Distance* is employed to quantify the existence of a novelty in

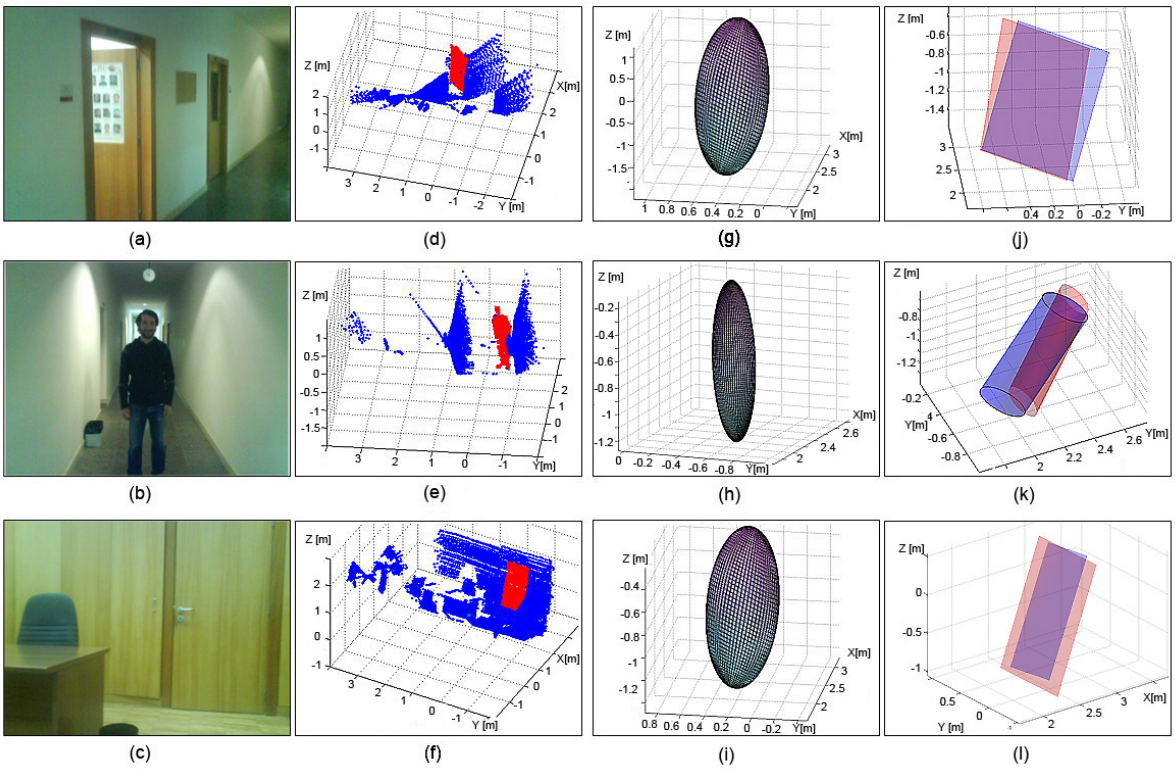


Fig. 6. Real data for testing the shape retrieval algorithms: a-c) Test areas for the real experiments described in the proposed approach; d-f) Real observations from an Hokuyo laser range finder (3-dimensions); and g-i) Gaussian functions associated to the novelty detected by the algorithm; and j-l) Shapes generated by the algorithms (red: method based on Mathematical space of Gaussian mixture; blue: method based on Euclidean space).

the scenario. Besides, this paper has developed two different methods to obtain geometric primitives of these changes in the environment. First, new samplings are generated from each Gaussian function associated to the novelty, followed of a RANSAC algorithm to retrieve geometric primitives. On the other hand, a new algorithm is developed to directly retrieve the shape according to the GMM information, that is, covariance and mean values associated to each novelty. In this paper the set of geometric primitives have been limited to the set $C = \{sphere, cylinder, plane\}$. Both two shape retrieval methods are compared, computational cost and accuracy of the retrieval shape are obtained. Experimental results in various real and simulated scenarios demonstrate the feasibility of the approach.

Future work will be focused on the extension of the set of geometric primitives (e.g. cones or boxes) or more complex structures. The final goal of the work is to obtain a whole system capable of detecting and representing virtual objects in the robot's world.

## REFERENCES


[1] S. Thrun, W. Burgard, and D. Fox. "Probabilistic Robotics". *MIT Press*, ISBN 0-262-20162-3, 2005.

[2] R. Rocha, F. Ferreira, and J. Dias. "Multi-robot complete exploration using hill climbing and topological recovery". In *Proc. of 2008 IEEE/RSJ Int. Conf. on Intelligent Robots and Systems* (IROS 2008), pp. 1884–1889, Nice, France, Sep. 2008.

[3] I. Amorim, R. Rocha, and J. Dias. "Mobile Robotic Surveillance Systems: Detecting and Evaluating Changes in 3D Mapped Environments". In *Proc. of 2nd Israeli Conference on Robotics* (ICR2008), Herzlia, Israel, Nov. 19-20, 2008.

[4] H. Andreasson, M. Magnusson, and A. Lilienthal. "Has something changed here? Autonomous Difference Detection for Security Patrol Robots". In *Proc. of IEEE/RSJ Int. Conf. on Intelligent Robots and Systems*, pp. 3429–3435, San Diego, USA, 2007.

[5] R. Schnabel, R. Wahl and R. Klein, "Efficient RANSAC for Point-Cloud Shape Detection", in *Computer Graphics Forum* , Volume 26, Number 2, June 2007 , pp. 214-226(13).

[6] D. Fox. "Markov localization for mobile robots in dynamic environments", *Journal of Artificial Intelligence Research*. Vol. 11, pages 391–427, 1999.

[7] P. Núñez, R. Vázquez-Martín, A. Bandera and F. Sandoval. "CF-IDC: A robust robot's self-localization in dynamic environments using curvature information", in *the 14th Mediterranean Electrotechnical Conference* (MELECON08), pp. 330–336, 2008.

[8] D. H. Ballard. "Generalizing the Hough transform to detect arbitrary shapes". *Pattern Recognition*, Vol. 13, n. 2, pp. 111–122, 1981.

[9] M. Vieria and K. Shimada. "Surface mesh segmentation and smooth surface extraction through region growing", *Computer Aided Geometric Design*, Vol. 22, No. 8, pp. 771-792, 2005.

[10] R. Wahl, M. Guthe and R. Klein, "Identifying planes in point-clouds for efficient hybrid rendering", in *the 13th Pacific Conference on Computer Graphics and Applications*, October 2005.

[11] J. Tangelder and R. Veltkamp, "A survey of content based 3D shape retrieval methods", in *Proceedings of the Shape Modeling International 2004*, IEEE computer Society, pp. 145–156, 2004.

[12] P. Pekka and J. K. Kamarainen, J. Ilonen and H. Kälviäinen. "Feature representation and discrimination based on Gaussian mixture model probability densities-Practices and algorithms", *Pattern Recogn.*, Vol. 39, pp. 1346–1358, 2006.

[13] C. Tomasi, Y. Rubner and L. J. Guives. "A metric for distributions with applications to image databases", in *Proc. of the 1998 IEEE International Conference on Computer Vision*, pp. 59–66, 1998.

[14] W. Forstner and B. Moonen, "A metric for covariance matrices", in *Technical Report, Dpt. of Geodesy and Geoinformatics*, University of Stuttgart, Germany, 1999.